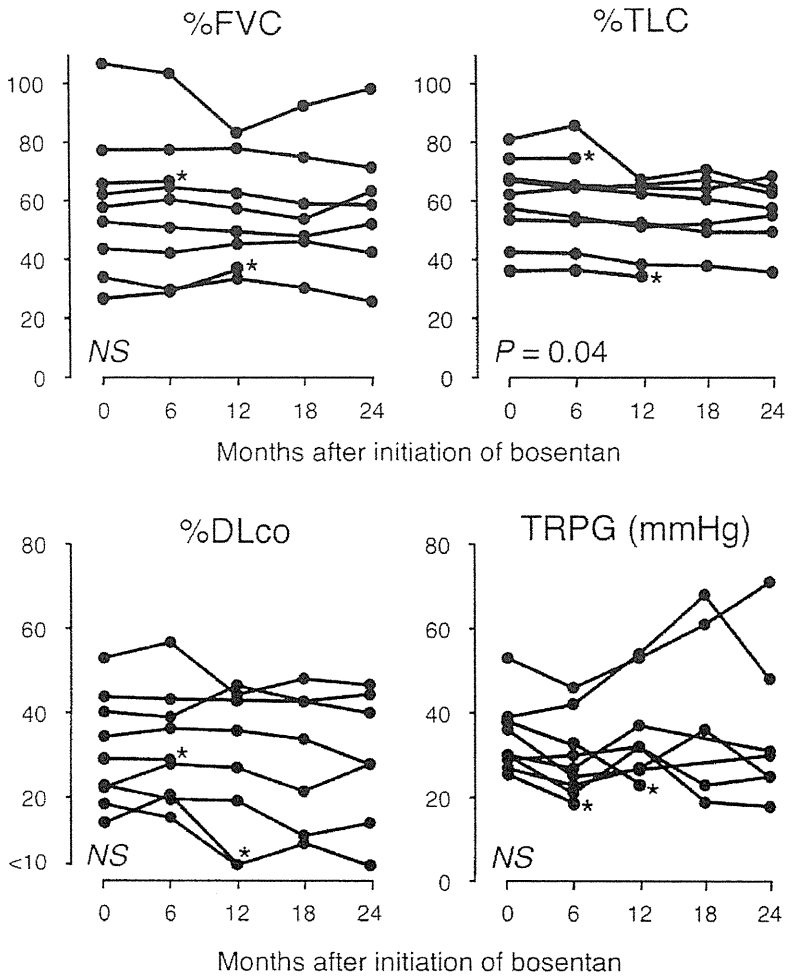

Figure 1. Pulmonary function test results and tricuspid regurgitation pressure gradient (TRPG) changes in 9 patients with SSc-ILD during treatment with bosentan. Statistical analysis was performed for the 7 patients who completed the 24-month study period. *Results from dropout patients. FVC: forced vital capacity; TLC: total lung capacity; DLCO: diffusing capacity for carbon monoxide; NS: not significant.

Table 2. Serial measurements of high resolution computed tomography (HRCT) scores, and measurements of skin thickening, peripheral vascular disease, and functional status in 7 patients who completed the entire study period. Results are shown as the mean ± SD.

Feature	Pretreatment	12 Months	24 Months	p
HRCT scores				
Ground-glass opacity	5.4 ± 4.0	6.1 ± 3.9	5.7 ± 3.5	0.2
Pulmonary fibrosis	8.3 ± 2.4	9.3 ± 2.8	9.1 ± 2.2	0.052
Honeycomb cysts	2.1 ± 3.1	3.0 ± 3.1	4.5 ± 3.7	0.02
Modified Rodnan skin score	13.9 ± 11.6	12.6 ± 9.8	12.7 ± 9.8	0.9
Oral aperture, mm	40.9 ± 13.6	38.9 ± 12.1	43.1 ± 10.8	0.6
FTP, right, mm	1.3 ± 1.3	1.5 ± 2.5	1.7 ± 1.9	0.5
Raynaud's condition score	2.6 ± 2.3	3.5 ± 2.8	3.3 ± 2.5	0.6
No. digital ulcers	0.9 ± 2.3	0.0 ± 0.0	0.1 ± 0.4	0.4
SHAQ-DI	0.7 ± 0.8	0.7 ± 0.9	0.8 ± 0.8	0.4
SHAQ-VAS	1.3 ± 0.5	1.2 ± 0.8	1.4 ± 0.6	0.7

FTP: finger tip-to-palm distance; SHAQ: Scleroderma Health Assessment Questionnaire; DI: disability index; VAS: visual analog scale.

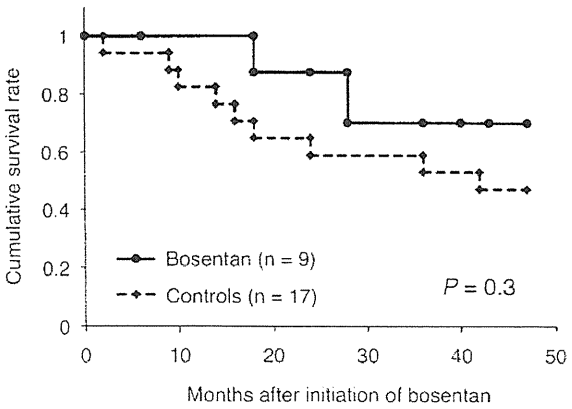

Figure 2. Cumulative survival rates in 9 patients treated with bosentan and 17 historical controls. Comparison between the 2 groups by Cox-Mantel log-rank test.

lier (Patient 9) with very long disease duration (338 months) and preserved %FVC (107%) was excluded from the bosentan-treated groups, disease duration and %FVC were 117 ± 134 and 52.0 ± 17.4, respectively, which were compatible to those in the historical controls. The reasons we did not treat ILD in 17 historical controls included severely impaired lung function in 11, long disease duration in 3, relapse after CYC treatment in 2, and recent malignancy in 1. Nine (53%) of the historical controls died within 48 months, and causes of death were all ILD-related, such as respiratory failure and respiratory tract infection. Although there was a trend toward better cumulative survival rates in the patients treated with bosentan, the difference did not reach statistical significance (p = 0.3). When an outlier (Patient 9) was excluded from the bosentan-treated group, cumulative survival rates at 3 years were almost concordant between bosentan-treated and control groups (67% vs 58%, respectively; p = 0.6).

DISCUSSION

Since the BUILD-2 trial had shown that bosentan does not reduce the frequency of clinically important worsening in SSc patients with active and progressive ILD[17], this prospective open-label study targeted the treatment of CYC-ineligible SSc-ILD. We found that 2-year treatment with bosentan did not have any beneficial effects on lung function or HRCT findings in the target population. Although bosentan was safe and well tolerated, all the outcome variables related to the extent and degree of ILD tended to worsen in spite of bosentan treatment. The relatively slow rate of progression in lung function changes and the HRCT findings in patients treated with bosentan were similar to the natural course of SSc-ILD[27]. Therefore, our data together with the BUILD-2 trial results do not support the use of bosentan as therapy for any forms of established ILD in patients with SSc, including the early disease with exertional dyspnea (SSc duration < 3 years), late active disease (SSc duration ≥ 3 years), or advanced or end-stage disease.

The majority of the patients enrolled in our study had extensive disease, above 20% on HRCT, and the predicted 4-year survival rate of this population was < 60%[22]. In addition, severely impaired lung function requiring oxygen supplementation, ILD concomitant with PH, and relapse after CYC treatment, which were observed in the majority of our patients, are associated with poor prognosis[28,29,30]. Our data showed clearly that bosentan did not improve lung function, but it is still possible that bosentan slowed the lung function deterioration in a patient population highly likely to have poor prognosis. Unfortunately, this issue cannot be evaluated in the setting of a 24-month noncomparative study involving a small number of patients. Our life-table analysis suggests that bosentan may prolong survival in comparison with historical controls, but we have to consider that historical controls might have developed a greater amount of lung deterioration in a shorter period of time in comparison with bosentan-treated patients because of shorter disease duration and lower %FVC. Moreover, historical controls included patients referred to our hospital before 2000, and this may contribute to poor survival

Table 3. Baseline characteristics of bosentan-treated patients and historical controls.

Characteristic	Bosentan-treated Patients, n = 9	Controls, n = 17	p
Years at study entry	2006–2007	1988–2006	
Age at study entry, yrs*	55.1 ± 19.0	54.3 ± 11.8	0.9
Women, %	56	71	0.7
Disease duration, mo*	141 ± 134	109 ± 52	0.4
Diffuse cutaneous SSc, %	56	88	0.3
Extensive disease (ILD staging), %	89	100	0.7
% FVC*	58.2 ± 24.4	50.8 ± 6.3	0.3
% DLCO	31.2 ± 12.5	31.1 ± 6.5	1.0
Oxygen supplementation, %	44	41	0.8
Pulmonary hypertension, %	11	18	0.9
Antitopoisomerase I antibody, %	56	82	0.3
Anti-U1RNP antibody, %	33	12	0.4

* Results are mean ± SD.

rates in historical controls because of outdated equipment and supportive therapies. Larger randomized controlled trials are needed to draw a final conclusion on whether bosentan treatment has some degree of benefit in patients with advanced or endstage ILD.

The potential benefit of ERA to suppress or prevent PH is particularly relevant in patients with SSc-ILD, because these agents have been confirmed to benefit SSc patients with PAH[11]. In this regard, it has been reported that in spite of ERA use, patients with ILD-associated PH have a 5-fold greater risk of death than those with PAH[29], disfavoring the efficacy of ERA in patients with PH owing to ILD. On the other hand, in the subanalysis of the BUILD-2 study assessing bosentan's preventive effect on PH in patients with SSc-ILD, PH developed in 5 patients (5.8%) in the placebo group, but in only one (1.3%) in the bosentan group during a 1-year study period, although this difference did not reach statistical significance[17]. However, in our study, 2 patients (22%) developed PH while being treated with bosentan. Thus, bosentan's efficacy for treating ILD-related PH is apparently inferior to its efficacy for treating PAH.

ET-1 is involved in many pathologic processes, including vasoconstriction, cell proliferation, and promotion of inflammation and fibrosis, and thus blocking ET-1 signaling may result in pleiotropic effects beyond vasodilation. These effects are expected to be beneficial in various aspects of SSc pathogenesis, making ERA attractive potential disease-modifying agents for SSc[31]. Two randomized, prospective, placebo-controlled studies (RAPIDS-1 and -2) have demonstrated that fewer digital ulcers develop in patients treated with bosentan than in those receiving a placebo, although ulcers did not appear to heal better with bosentan treatment[32,33]. Recent open-label studies have shown that bosentan is potentially effective for reducing skin thickening in patients with SSc[34,35]. In contrast, we did not observe any improvement in outcome measures associated with Raynaud's phenomenon, skin thickening, or functional status during bosentan treatment. These negative findings were also reported in the BUILD-2 trial[17]. The lack of therapeutic responses to bosentan may argue against a critical role for ET-1 in SSc pathogenesis, but it is also possible that because of the established and advanced stages of disease in our patient population any effective timing of treatment (in terms of the reversibility of the pathogenic process) might already have passed.

Treatment with bosentan did not improve or stabilize lung function in SSc patients with advanced ILD. Currently, there is no evidence to recommend the use of endothelin receptor antagonists for treating SSc-ILD, even when the disease is ineligible for CYC treatment.

REFERENCES

1. White B. Interstitial lung disease in scleroderma. Rheum Dis Clin North Am 2003;29:371-90.
2. Steen VD, Medsger TA. Changes in causes of death in systemic sclerosis, 1972-2002. Ann Rheum Dis 2007;66:940-4.
3. Tashkin DP, Elashoff R, Clements PJ, Goldin J, Roth MD, Furst DE, et al. Cyclophosphamide versus placebo in scleroderma lung disease. N Engl J Med 2006;354:2655-66.
4. Tashkin DP, Elashoff R, Clements PJ, Goldin J, Roth MD, Furst DE, et al. Effects of 1-year treatment with cyclophosphamide on outcomes at 2 years in scleroderma lung disease. Am J Respir Crit Care Med 2007;176:1026-34.
5. Nannini C, West CP, Erwin PJ, Matteson EL. Effects of cyclophosphamide on pulmonary function in patients with scleroderma and interstitial lung disease: a systematic review and meta-analysis of randomized controlled trials and observational prospective cohort studies. Arthritis Res Ther 2008;10:R124.
6. Broad K, Pope JE. The efficacy of treatment for systemic sclerosis interstitial lung disease: results from a meta-analysis. Med Sci Monit 2010;16:RA187-90.
7. Khanna D, Furst DE, Clements PJ, Tashkin DP, Eckman MH. Oral cyclophosphamide for active scleroderma lung disease: a decision analysis. Med Decis Making 2008;28:926-37.
8. Au K, Khanna D, Clements PJ, Furst DE, Tashkin DP. Current concepts in disease-modifying therapy for systemic sclerosis-associated interstitial lung disease: lessons from clinical trials. Curr Rheumatol Rep 2009;11:111-9.
9. Peacock AJ, Dawes KE, Shock A, Gray AJ, Reeves JT, Laurent GJ. Endothelin-1 and endothelin-3 induce chemotaxis and replication of pulmonary artery fibroblasts. Am J Respir Cell Mol Biol 1992;7:492-9.
10. Rubin LJ, Badesch DB, Barst RJ, Galie N, Black CM, Keogh A, et al. Bosentan therapy for pulmonary arterial hypertension. N Engl J Med 2002;346:896-903.
11. Denton CP, Pope JE, Peter HH, Gabrielli A, Boonstra A, van den Hoogen FH, et al. Long-term effects of bosentan on quality of life, survival, safety and tolerability in pulmonary arterial hypertension related to connective tissue diseases. Ann Rheum Dis 2008;67:1222-8.
12. Shi-Wen X, Denton CP, Dashwood MR, Holmes AM, Bou-Gharios G, Pearson JD, et al. Fibroblast matrix gene expression and connective tissue remodeling: role of endothelin-1. J Invest Dermatol 2001;116:417-25.
13. Lagares D, García-Fernández RA, Jiménez CL, Magán-Marchal N, Busnadiego O, Lamas S, et al. Endothelin-1 contributes to the effect of transforming growth factor-ß1 on wound repair and skin fibrosis. Arthritis Rheum 2010;62:878-89.
14. Reichenberger F, Schauer J, Kellner K, Sack U, Stiehl P, Winkler J. Different expression of endothelin in the bronchoalveolar lavage in patients with pulmonary diseases. Lung 2001;179:163-74.
15. Park SH, Saleh D, Giaid A, Michel RP. Increased endothelin-1 in bleomycin-induced pulmonary fibrosis and the effect of an endothelin receptor antagonist. Am J Respir Crit Care Med 1997;156:600-8.
16. King TE Jr, Behr J, Brown KK, du Bois RM, Lancaster L, de Andrade JA, et al. BUILD-1: a randomized placebo-controlled trial of bosentan in idiopathic pulmonary fibrosis. Am J Respir Crit Care Med 2008;177:75-81.
17. Seibold JR, Denton CP, Furst DE, Guillevin L, Rubin LJ, Wells A, et al. Randomized, prospective, placebo-controlled trial of bosentan in interstitial lung disease secondary to systemic sclerosis. Arthritis Rheum 2010;62:2101-8.
18. Masi AT, Rodnan GP, Medsger TA Jr, Altman RD, D'Angelo WA, Fries JF, et al. Preliminary criteria for the classification of systemic sclerosis (scleroderma). Arthritis Rheum 1980;23:581-90.
19. Medsger TA Jr. Systemic sclerosis (scleroderma): clinical aspects. In: Koopman WJ, editor. Arthritis and allied conditions. 13th ed. Baltimore: Williams & Wilkins; 1997:1433-64.
20. Galiè N, Hoeper MM, Humbert M, Torbicki A, Vachiery JL, Barbera JA, et al. Guidelines for the diagnosis and treatment of

pulmonary hypertension: the Task Force for the Diagnosis and Treatment of Pulmonary Hypertension of the European Society of Cardiology (ESC) and the European Respiratory Society (ERS), endorsed by the International Society of Heart and Lung Transplantation (ISHLT). Eur Heart J 2009;30:2493-537.
21. Goldin JG, Lynch DA, Strollo DC, Suh RD, Schraufnagel DE, Clements PJ, et al. High-resolution CT scan findings in patients with symptomatic scleroderma-related interstitial lung disease. Chest 2008;134:358-67.
22. Goh NS, Desai SR, Veeraraghavan S, Hansell DM, Copley SJ, Maher TM, et al. Interstitial lung disease in systemic sclerosis: a simple staging system. Am J Respir Crit Care Med 2008;177:1248-54.
23. Merkel PA, Herlyn K, Martin RW, Anderson JJ, Mayes MD, Bell P, et al. Measuring disease activity and functional status in patients with scleroderma and Raynaud's phenomenon. Arthritis Rheum 2002;46:2410-20.
24. Steen VD, Medsger TA Jr. The value of the Health Assessment Questionnaire and special patient-generated scales to demonstrate change in systemic sclerosis patients over time. Arthritis Rheum 1997;40:1984-91.
25. Kuwana M, Sato S, Kikuchi K, Kawaguchi Y, Fujisaku A, Misaki Y, et al. Evaluation of functional disability using the Health Assessment Questionnaire in Japanese patients with systemic sclerosis. J Rheumatol 2003;30:1253-8.
26. Kuwana M, Kaburaki J, Okano Y, Tojo T, Homma M. Clinical and prognostic associations based on serum antinuclear antibodies in Japanese patients with systemic sclerosis. Arthritis Rheum 1994;37:75-83.
27. Wells AU, Cullinan P, Hansell DM, Rubens MB, Black CM, Newman-Taylor AJ, et al. Fibrosing alveolitis associated with systemic sclerosis has a better prognosis than lone cryptogenic fibrosing alveolitis. Am J Respir Crit Care Med 1994;149:1583-90.
28. Medsger TA Jr, Silman AJ, Steen VD, Black CM, Akesson A, Bacon PA, et al. A disease severity scale for systemic sclerosis: development and testing. J Rheumatol 1999;26:2159-67.
29. Mathai SC, Hummers LK, Champion HC, Wigley FM, Zaiman A, Hassoun PM, et al. Survival in pulmonary hypertension associated with the scleroderma spectrum of diseases: impact of interstitial lung disease. Arthritis Rheum 2009;60:569-77.
30. Furst DE, Khanna D, Clements PJ, Sullivan K, Tashkin DP. Serious complications and mortality among 158 patients with systemic sclerosis (SSc) in the Scleroderma Lung Study (SLS) followed for up to 9 years [abstract]. Arthritis Rheum 2010;62 Suppl:2194.
31. Shetty N, Derk CT. Endothelin receptor antagonists as disease modifiers in systemic sclerosis. Inflamm Allergy Drug Targets 2011;10:19-26.
32. Korn JH, Mayes M, Matucci-Cerinic M, Rainisio M, Pope J, Hachulla E, et al. Digital ulcers in systemic sclerosis: prevention by treatment with bosentan, an oral endothelin receptor antagonist. Arthritis Rheum 2004;50:3985-93.
33. Matucci-Cerinic M, Denton CP, Furst DE, Mayes MD, Hsu VM, Carpentier P, et al. Bosentan treatment of digital ulcers related to systemic sclerosis: results from the RAPIDS-2 randomised, double-blind, placebo-controlled trial. Ann Rheum Dis 2011;70:32-8.
34. Kuhn A, Haust M, Ruland V, Weber R, Verde P, Felder G, et al. Effect of bosentan on skin fibrosis in patients with systemic sclerosis: a prospective, open-label, non-comparative trial. Rheumatology 2010;5:1-10.
35. Giordano N, Puccetti L, Papakostas P, Di Pietra N, Bruni F, Pasqui AL, et al. Bosentan treatment for Raynauds phenomenon and skin fibrosis in patients with systemic sclerosis and pulmonary arterial hypertension: an open-label, observational, retrospective study. Int J Immunopathol Pharmacol 2010;23:1185-94.

RHEUMATOLOGY

Rheumatology 2012;51:129–133
doi:10.1093/rheumatology/ker333
Advance Access publication 9 November 2011

Concise report

Investigation of prognostic factors for skin sclerosis and lung function in Japanese patients with early systemic sclerosis: a multicentre prospective observational study

Minoru Hasegawa[1], Yoshihide Asano[2], Hirahito Endo[3], Manabu Fujimoto[1], Daisuke Goto[4], Hironobu Ihn[5], Katsumi Inoue[6], Osamu Ishikawa[7], Yasushi Kawaguchi[8], Masataka Kuwana[9], Yoshinao Muro[10], Fumihide Ogawa[11], Tetsuo Sasaki[12], Hiroki Takahashi[13], Sumiaki Tanaka[14], Kazuhiko Takehara[1] and Shinichi Sato[2]

Abstract

Objective. To clarify the clinical course of SSc in Japanese patients with early-onset disease. It is well known that ethnic variations exist in the clinical features and severity of SSc. However, neither the clinical course nor prognostic factors have been thoroughly investigated in the Japanese population.

Methods. Ninety-three Japanese patients of early-onset SSc (disease duration: <3 years) with diffuse skin sclerosis and/or interstitial lung disease were registered in a multi-centre observational study. All patients had a physical examination with laboratory tests at their first visit and at each of the three subsequent years. Factors that could predict the severity of skin sclerosis and lung involvement were examined statistically by multiple regression analysis.

Results. Two patients died from SSc-related myocardial involvement and four patients died from other complications during the 3-year study. Among various clinical data assessed, the initial modified Rodnan total skin thickness score (MRSS) and maximal oral aperture were associated positively and negatively with MRSS at Year 3, respectively. Additionally, initial ESR tended to be associated with final MRSS. Pulmonary vital capacity (VC) in the third year was significantly associated with initial %VC. Furthermore, patients with anti-topo I antibody tended to show reduced %VC at Year 3.

Conclusions. Several possible prognostic factors for skin sclerosis and lung function were detected in Japanese patients with early SSc. Further longitudinal studies of larger populations will be needed to confirm these findings.

Key words: systemic sclerosis, scleroderma, prognostic factor, skin sclerosis, interstitial lung diseases, treatment

[1]Department of Dermatology, Kanazawa University Graduate School of Medical Science, Kanazawa, [2]Department of Dermatology, Faculty of Medicine, University of Tokyo, Tokyo, [3]Department of Internal Medicine (Omori), Toho University School of Medicine, Tokyo, [4]Department of Rheumatology, Graduate School of Comprehensive Human Sciences, University of Tsukuba, Tsukuba, [5]Department of Dermatology and Plastic Surgery, Faculty of Life Sciences, Kumamoto University, Kumamoto, [6]Division of Rehabilitation Science, Kanazawa University Graduate School of Medical Science, Kanazawa, [7]Department of Dermatology, Gunma University Graduate School of Medicine, Maebashi, [8]Institute of Rheumatology, Tokyo Women's Medical University, [9]Division of Rheumatology, Department of Internal Medicine, Keio University School of Medicine, Tokyo, [10]Department of Dermatology, Nagoya University Graduate School of Medicine, Nagoya, [11]Department of Dermatology, Nagasaki University Graduate School of Biomedical Science, Nagasaki, [12]Department of Dermatology, Atami Hospital, International University of Health and Welfare, Atami, [13]First Department of Internal Medicine, Sapporo Medical University School of Medicine, Sapporo and [14]Department of Rheumatology and Infectious Diseases, Kitasato University School of Medicine, Sagamihara, Japan.

Submitted 12 April 2011; revised version accepted 25 August 2011.

Correspondence to: Minoru Hasegawa, Department of Dermatology, Kanazawa University Graduate School of Medical Science, 13-1 Takaramachi, Kanazawa, Ishikawa 920-8641, Japan.
E-mail: minoruha@derma.m.kanazawa-u.ac.jp

Introduction

SSc is a CTD characterized by tissue fibrosis in the skin and internal organs. Interstitial lung diseases (ILDs) develop in more than half of SSc patients and are one of the major SSc-related causes of death [1, 2]. The natural course of skin sclerosis and internal organ involvement and identification of prognostic factors have been extensively reported in Europe and the USA [3–6]. However, there are some racial differences in the clinical and laboratory features of SSc [7]. For example, the severity of skin sclerosis is modest in Japanese patients [8]. Furthermore, pulmonary arterial hypertension and renal crisis are rare in Japanese SSc patients [9]. Furthermore, racial differences are found in the distribution of SSc-related serum ANAs [10]. The frequency of anti-RNA polymerases antibody (Ab) is lower in the Japanese population than in US or European patient populations [9]. However, there have been no multiple-centre prospective studies concerning the clinical features of SSc in Japanese individuals.

In most patients, severe organ involvement occurs within the first 3 years of disease and skin sclerosis seldom progresses after 5 or 6 years [3, 11]. Therefore, predicting disease progression is particularly important for SSc patients at their first visit. In the present study, we aimed to determine if any initial clinical or laboratory features were associated with subsequent disease severity in Japanese SSc patients with a short disease duration of <3 years.

Materials and methods

Patients

Patients were grouped according to the degree of skin involvement, based on the classification system proposed by LeRoy *et al.* (dcSSc *vs* lcSSc) [12]. In this study, 93 Japanese patients with early SSc (disease duration: <3 years) who had dcSSc or ILD were registered at 12 major scleroderma centres in Japan (Atami Hospital, International University of Health and Welfare; Gunma University Hospital; Kanazawa University Hospital; Keio University Hospital; Kitasato University Hospital; Kumamoto University Hospital; Nagasaki University Hospital; Nagoya University Hospital; Sapporo Medical University Hospital; Tokyo University Hospital; Tokyo Women's Medical University Hospital; Tsukuba University Hospital).

Among these patients, two died from SSc-related myocardial involvement and four died from complications (ANCA-associated vasculitis, sepsis, thrombotic thrombocytopenic purpura and uterine cancer, respectively) during the 3-year study. Therefore, 87 patients (49 patients had dcSSc with ILD, 27 patients had dcSSc without ILD and 11 patients had lcSSc with ILD) were followed for 3 years. Sixty-four were females and 23 were males; the median (range) age was 50 (3–74) years. All patients fulfilled the criteria for SSc proposed by the ACR [13]. The median (range) disease duration (the period from the development of any symptoms excluding RP to our first assessment) of patients was 20 (1–35) months. With respect to ANA, 56 patients were positive for anti-topo I Ab and 7 patients were positive for ACA. Medical ethics committee of Kanazawa University approved the study. In addition, this study was approved by the ethics committees of International University of Health and Welfare, Gunma University, Keio University, Kitasato University, Kumamoto University, Nagasaki University, Nagoya University, Sapporo Medical University, Tokyo University, Tokyo Women's Medical University and Tsukuba University. Informed consent was obtained from all patients.

Clinical assessments

Patients had a physical examination and laboratory tests performed at their first visit and at each subsequent year for 3 years. The degree of skin involvement was determined according to the modified Rodnan total skin thickness score (MRSS), as described elsewhere [14]. Organ system involvement was defined as described previously [15] with some modifications: ILD = bibasilar interstitial fibrosis or ground-glass shadow on high-resolution CT (HRCT); pulmonary arterial hypertension (PAH) = clinical evidence of pulmonary hypertension and elevated right ventricular systolic pressure (>45 mmHg) documented by echocardiography in the absence of severe pulmonary interstitial fibrosis; oesophagus = apparent dysphasia, reflux symptoms or hypomotility shown by barium radiography; heart = pericarditis, congestive heart failure or arrhythmias requiring treatment; kidney = malignant hypertension and rapidly progressive renal failure unexplained by certain diseases other than SSc; joint = inflammatory polyarthralgias or arthritis; and muscle = proximal muscle weakness and elevated serum creatine kinase. An HAQ modified for Japanese patients [16], digital ulcer, pitting scar, maximal oral aperture (the maximum vertical length of opened mouth) and skin pigmentation/depigmentation were also evaluated. ESR and pulmonary function, including vital capacity (VC) and diffusion capacity for carbon monoxide (DL_{CO}) were also tested.

Statistical analysis

JMP Statistically Discovery Software (SAS institute, Cary, NC, USA) was used for analysis. Potential prognostic factors for the severity of skin sclerosis and lung function were statistically examined by multiple regression analysis. A $P < 0.05$ was considered to be statistically significant. All values are expressed as the median (range).

Results

The clinical course of SSc in Japanese patients

To provide a comprehensive evaluation of the clinical features of SSc in Japanese patients, we analysed clinical data as well as laboratory test results from 87 patients with short disease duration (Table 1). To assess the degree of skin involvement in patients, MRSS values were calculated; VC and DL_{CO} percentages were used to assess lung involvement. For the patient population as a whole, the median (range) MRSS decreased from 17 (2–42) to 12 (0–41) during the first year. The median (range) MRSS

was 12 (0–41) at the end of Year 2 and 10 (0–47) at the end Year 3. Median (range) values for %VC did not significantly change during the 3-year evaluation period: 95 (49–144) at first visit, 93 (26–137) at the end of the first year, 95 (49–144) at the end of the second year and 92 (51–137) at the end of the third year. Similarly, median values for % DL_{CO} did not significantly change during the 3 years.

The frequency of patients with ILD or PAH was stable during the evaluation period. Similarly, the number of patients with oesophageal or joint involvement, pitting scar or skin pigmentation/depigmentation did not vary significantly over time. The value of HAQ and maximal oral aperture did not significantly change during the course. The median (range) value of ESR was 18 (2–95) mm/h at the first visit, then it reduced to 16 (2–84), 13 (1–63) and 12 (0.5–122) mm/h, during the subsequent 3 years. Oral prednisolone (~20 mg/day) use was common, with 56 patients starting to take this drug after the first visit and 70 patients having taken it by the end of Year 3. Two patients developed renal crisis during the course of the study (data not shown). Patients with digital ulcer or heart or muscle involvement were rare during the course (fewer than 10 patients, data not shown).

Prognostic factors of the progress of skin sclerosis

Next, we evaluated clinical or laboratory factors presenting at first visit that could predict the severity of skin sclerosis of 3 years later. Investigated factors were as follows: age, gender, disease duration, anti-topo I Ab, ACA, MRSS at the first visit, %VC, % DL_{CO}, existence of each organ involvement (ILD, PAH, oesophagus, joint), pitting scar, skin pigmentation/depigmentation, HAQ, maximal oral aperture, ESR, CS treatment and cyclophosphamide treatment. Cases that have any missing data were excluded and thereby 80 patients were analysed. We performed multiple regression using stepwise way that specified the α-level for either adding or removing a regression as 0.20 (Table 2). As a result, the multiple regression equation predicting MRSS at the third year = 17.11 + 0.35 × MRSS at the first visit + −0.26 × maximal oral aperture + 0.042 × ESR ($R^2 = 0.63$, $P < 0.0001$). Thus, MRSS at the third year was significantly associated with MRSS at first visit ($P < 0.001$) and was negatively associated with initial maximal oral aperture at first visit ($P < 0.01$). Additionally, initial ESR tended to be associated with final MRSS ($P = 0.17$).

Prognostic factors of lung function

We similarly assessed the prognostic factors of impaired lung function to estimate ILD severity. Here, we used %VC as representative markers of lung function. Cases that have any missing data including %VC at the third year were excluded and thereby 58 patients were analysed. We performed multiple regression in a stepped manner that specified the α-level for either adding or removing a regression as 0.20 (Table 3). As a result, the multiple regression equation predicting %VC at the third

Table 2 Factors predicting MRSS at the third year determined by multiple regression analysis

	Estimate	Standard error	*P*-value
Intercept	17.11	4.88	<0.01
MRSS at the first visit	0.35	0.089	<0.001
Maximal oral aperture	−0.26	0.075	<0.01
ESR	0.042	0.043	0.17

The multiple regression equations predicting MRSS at the third year are as follows; MRSS at the third year = 17.11 + 0.35 × MRSS at the first visit + −0.26 × maximal oral aperture + 0.042 × ESR. R^2 (determination coefficient) = 0.63; Root mean square error = 4.73; $P < 0.0001$.

Table 1 The course of clinical and laboratory features in patients with SSc

	First visit	Year 1	Year 2	Year 3
MRSS	17 (2–42); *n* = 87	12 (0–41); *n* = 84	12 (0–41); *n* = 84	10 (0–47); *n* = 87
%VC	95 (49–144); *n* = 70	93 (26–137); *n* = 55	95 (49–144); *n* = 57	92 (51–137); *n* = 60
% DL_{CO}	70 (11–113); *n* = 70	68 (10–105); *n* = 55	69 (11–96); *n* = 57	68 (10–120); *n* = 60
ILD	54 (62); *n* = 87	47 (64); *n* = 73	47 (64); *n* = 73	46 (63); *n* = 73
PAH	9 (10); *n* = 87	9 (12); *n* = 76	8 (11); *n* = 72	11 (13); *n* = 84
Oesophagus	33 (37); *n* = 87	26 (34); *n* = 77	35 (48); *n* = 73	34 (40); *n* = 85
Joint	20 (23); *n* = 86	14 (18); *n* = 77	9 (12); *n* = 73	17 (20); *n* = 84
Pitting scar	27 (33); *n* = 87	29 (38); *n* = 76	35 (48); *n* = 73	33 (38); *n* = 86
Pigmentation/depigmentation	54 (62); *n* = 87	49 (64); *n* = 77	41 (57); *n* = 72	50 (60); *n* = 84
HAQ	0.08 (0–2); *n* = 83	0.125 (0–1.75); *n* = 74	0.25 (0–2.5); *n* = 73	0.125 (0–2.25); *n* = 83
Maximal oral aperture	45 (18–70); *n* = 87	45 (28–65); *n* = 75	46 (25–67); *n* = 72	45 (10–67); *n* = 83
ESR	18 (2–95); *n* = 80	16 (2–84); *n* = 61	13 (1–63); *n* = 52	12 (0.5–122); *n* = 57
CS	56 (64); *n* = 87	61 (82); *n* = 74	64 (86); *n* = 74	70 (80); *n* = 87
Cyclophosphamide	11 (13); *n* = 87	14 (19); *n* = 75	8 (12); *n* = 68	9 (10); *n* = 87

Values are represented as median (range) or as number of positive cases with percentage within parentheses, in total patients in whom those data are available.

TABLE 3 Factors predicting %VC at the third year determined by multiple regression analysis

	Estimate	Standard error	*P*-value
Intercept	10.94	8.54	0.20
%VC at the first visit	0.85	0.09	<0.0001
Anti-topo I Ab (+)	2.32	1.64	0.19

The multiple regression equations predicting %VC at the third year are as follows: %VC at the third year = 10.94 + 0.85 × %VC at the first visit + anti-topo I Ab ('+' → −2.32, '−' → 2.32). $R^2 = 0.70$; Root mean square error = 12.00; $P < 0.0001$.

year = 10.94 + 0.85 × %VC at the first visit + anti-topo I Ab ('+' → −2.32, '−' → 2.32) ($R^2 = 0.70$, $P < 0.0001$). Thus, %VC at the third year was significantly associated with the value of %VC at first visit ($P < 0.0001$). In addition, %VC at the third year tended to be lower in patients with anti-topoisomerase I Ab ($P = 0.19$).

Discussion

To our knowledge, this study is the first multiple-centre, longitudinal prospective study to investigate the clinical course of Japanese patients. For this study, 87 patients with early-onset SSc (<3 years) were followed over 3 years. Median MRSS was reduced 5 points during the first year, and continued to decrease through the third year. This trend was similar to that identified in our previous, single-centre prospective observational study of Japanese SSc patients [17]. Although the reason for the prominent first-year reduction in MRSS in our current study is unknown, our previous single-centre study [17] indicated that the dose of oral CS was related to the decrease of MRSS. However, in this multi-centre observational study we could not perform a similar analysis of prednisolone dose in patients at each centre. In addition, other therapies including cyclophosphamide were also used in a part of patients in our observational study. Previous large studies demonstrated that MRSS naturally reduced during the disease course and time was a significant predictor of MRSS [3–6]. Therefore, the effect of CS therapy for MRSS remains unclear from our data. Since it has been suggested that CS therapy can induce renal crisis, high doses of CSs have not been recommended for the treatment of SSc [18]. However, renal crisis is not as common in Japanese patients [9], and only two patients (one had been taking low-dose CS, whereas the other had not) developed renal crisis during the course of our study.

The main aim of this study was to define the prognostic factors of skin sclerosis and ILD. The multiple regression equation was defined to predict the MRSS at the third year among multiple factors presenting at the first visit. MRSS at the first visit was significantly correlated with MRSS at the third year in all patients. Maximal oral aperture was correlated inversely with MRSS in the third year. Thus, the current skin sclerosis likely reflects the extent of skin sclerosis of 3 years later independent of other organ's involvement or treatment. Additionally, ESR tended to be associated with final MRSS. The presence of autoantibodies such as anti-topo I Ab and ACA was not shown to have value as a prognostic indicator of MRSS. However, this may be due to population bias in our study, since most patients were positive for anti-topo I Ab and negative for ACA.

The current study revealed that %VC and $\%DL_{CO}$ remained nearly constant or slightly reduced during the 3-year period. Since patients with progressive ILD received immunosuppressive treatment, including cyclophosphamide therapy in the participating facilities, this may have affected the stabilization of lung function in our cases. The frequency of ILD detected by HRCT was not increased during the course of the study, indicating ILD is usually detected early in the disease course and rarely develops later. In consistent with generally stable course of %VC, %VC at their first visit highly associated with the %VC at the third year in all patients with or without treatment. Patients with anti-topo I Ab tended to show reduced %VC at the third year. Although these findings are not surprising, we first confirmed them in Japanese patients.

Our study has some limitations. The population is not large and the follow-up period is not long. This is an observational study and therefore the treatment is heterogeneous. In addition, other parameters including CRP could not be analysed due to the lack of data. We should also include disease activity variables [19] and disease severity scale [20] in our future study. Further longitudinal studies in a larger population will be needed to clarify the natural course and prognostic factors in Japanese SSc patients.

Rheumatology key messages

- Initial ESR tended to be associated with skin score at Year 3 in Japanese scleroderma patients.
- Japanese scleroderma patients with anti-topo I Ab tended to show reduced %VC at the third year.

Acknowledgements

The manuscript has not been previously published nor has it been submitted simultaneously for publication elsewhere. We are grateful to all the physicians who have contributed in assembling the data at each facility. We also thank Tomoko Hayashi and Yuko Yamada for their assistance in registering data.

Funding: This work was supported by funds for research on intractable diseases from the Ministry of Health, Labor, and Welfare of Japan.

Disclosure statement: The authors have declared no conflicts of interest.

References

1 Silver RM. Clinical problems: the lungs. Rheum Dis Clin Nor Am 1996;22:825–40.

2 Steen VD, Conte C, Owens GR, Medsger TA. Severe restrictive lung disease in systemic sclerosis. Arthritis Rheum 1994;37:1283–9.

3 Steen VD, Medsger TA Jr. Severe organ involvement in systemic sclerosis with diffuse scleroderma. Arthritis Rheum 2000;43:2437–44.

4 Tyndall AJ, Bannert B, Vonk M *et al*. Causes and risk factors for death in systemic sclerosis: a study from the EULAR Scleroderma Trials and Research (EUSTAR) database. Ann Rheum Dis 2010;69:1809–15.

5 Walker UA, Tyndall A, Czirjak L *et al*. Clinical risk assessment of organ manifestations in systemic sclerosis: a report from the EULAR Scleroderma Trials And Research group database. Ann Rheum Dis 2007;66:754–63.

6 Amjadi S, Maranian P, Furst DE *et al*. Course of the modified Rodnan skin thickness score in systemic sclerosis clinical trials: analysis of three large multicenter, double-blind, randomized controlled trials. Arthritis Rheum 2009;60:2490–8.

7 Laing TJ, Gillespie BW, Toth MB *et al*. Racial differences in scleroderma among women in Michigan. Arthritis Rheum 1997;40:734–42.

8 Nishioka K, Katayama I, Kondo H *et al*. Epidemiological analysis of prognosis of 496 Japanese patients with progressive systemic sclerosis (SSc). Scleroderma Research Committee Japan. J Dermatol 1996;23:677–82.

9 Hamaguchi Y, Hasegawa M, Fujimoto M *et al*. The clinical relevance of serum antinuclear antibodies in Japanese patients with systemic sclerosis. Br J Dermatol 2008;158:487–95.

10 Kuwana M, Okano Y, Kaburaki J *et al*. Racial differences in the distribution of systemic sclerosis-related serum antinuclear antibodies. Arthritis Rheum 1994;37:902–6.

11 Medsger TA Jr. Classification, purpose. In: Clements PJ, Furst DE, eds. Systemic Sclerosis. Philadelphia: Williams & Wilkins, 2004:17–28.

12 LeRoy EC, Krieg T, Black C *et al*. Scleroderma (systemic sclerosis): classification, subsets, and pathogenesis. J Rheumatol 1988;15:202–5.

13 Committee SfSCotARADaTC. Preliminary criteria for the classification of systemic sclerosis (scleroderma). Arthritis Rheum 1980;23:581–90.

14 Clements P, Lachenbrush P, Seibold J *et al*. Inter and intraobserver variability of total skin thickness score (modified Rodnan TSS) in systemic sclerosis. J Rheumatol 1995;22:1281–5.

15 Steen VD, Powell DL, Medsger TAJ. Clinical correlations and prognosis based on serum autoantibodies in patients with systemic sclerosis. Arthritis Rheum 1988;31:196–203.

16 Kuwana M, Sato S, Kikuchi K *et al*. Evaluation of functional disability using the health assessment questionnaire in Japanese patients with systemic sclerosis. J Rheumatol 2003;30:1253–8.

17 Hasegawa M, Fujimoto M, Matsushita T. Serum chemokine and cytokine levels as indicators of disease activity in patients with systemic sclerosis. Clin Rheumatol 2011;30:231–7.

18 Steen VD, Medsger TA Jr, Osial TA Jr. Factors predicting development of renal involvement in progressive systemic sclerosis. Am J Med 1984;76:779–86.

19 Valentini G, Della Rossa A, Bombardieri S *et al*. European multicentre study to define disease activity criteria for systemic sclerosis. II. Identification of disease activity variables and development of preliminary activity indexes. Ann Rheum Dis 2001;60:592–8.

20 Medsger TA Jr, Silman AJ, Steen VD *et al*. A disease severity scale for systemic sclerosis: development and testing. J Rheumatol 1999;26:2159–67.

Journal of Neuroscience Research

Journal of Neuroscience Research 90:479–488 (2012)

Intracranial Transplantation of Monocyte-Derived Multipotential Cells Enhances Recovery After Ischemic Stroke in Rats

Hidenori Hattori,[1] Shigeaki Suzuki,[1] Yuka Okazaki,[2] Norihiro Suzuki,[1] and Masataka Kuwana[2]*

[1]Department of Neurology, Keio University School of Medicine, Tokyo, Japan
[2]Division of Rheumatology, Department of Internal Medicine, Keio University School of Medicine, Tokyo, Japan

Cell transplantation has emerged as a potential therapy to reduce the neurological deficits caused by ischemic stroke. We previously reported a primitive cell population, monocyte-derived multipotential cells (MOMCs), which can differentiate into mesenchymal, neuronal, and endothelial lineages. In this study, MOMCs and macrophages were prepared from rat peripheral blood and transplanted intracranially into the ischemic core of syngeneic rats that had undergone a left middle cerebral artery occlusion procedure. Neurological deficits, as evaluated by the corner test, were less severe in the MOMC-transplanted rats than in macrophage-transplanted or mock-treated rats. Histological evaluations revealed that the number of microvessels that had formed in the ischemic boundary area by 4 weeks after transplantation was significantly greater in the MOMC-transplanted rats than in the control groups. The blood vessel formation was preceded by the appearance of round $CD31^+$ cells, which we confirmed were derived from the transplanted MOMCs. Small numbers of blood vessels incorporating MOMC-derived endothelial cells expressing a mature endothelial marker RECA-1 were detected at 4 weeks after transplantation. In addition, MOMCs expressed a series of angiogenic factors, including vascular endothelial growth factor, angiopoetin-1, and placenta growth factor (PlGF). These findings provide evidence that the intracranial delivery of MOMCs enhances functional recovery by promoting neovascularization in a rat model for ischemic stroke.

Key words: stroke; angiogenesis; transplantation; monocytes; macrophages

Cell transplantation is a potential therapy for improving functional capacity in patients with cerebral ischemia. Several cell types have been proposed as transplantable cells, based on improved outcomes in a rodent stroke model. For example, the intravenous administration of cultured bone marrow stromal cells, which exhibit the properties of multipotential stem cells, reduced neurological deficits in a rodent model of stroke (Chen et al., 2001a; Shen et al., 2007a,b). Bone marrow stromal cell transplantation was reported to be effective and safe in five stroke patients in Korea, although the preparation of a sufficient quantity of autologous bone marrow stromal cells required at least 1 month of ex vivo culture (Bang et al., 2005). On the other hand, the intravenous administration of cultured human endothelial progenitor cells resulted in improved neurobehavioral outcomes in adult nude mice with experimentally induced cerebral ischemia (Fan et al., 2010). Other proposed cell sources for transplantation include human umbilical cord blood cells (Chen et al., 2001b) and bone marrow mononuclear cells (MNCs; Iihoshi et al., 2004; Kamiya et al., 2008; Brenneman et al., 2010). One of the advantages of using these freshly prepared cells is the feasibility of transplantation immediately after cerebral ischemia, but the optimal route and timing of administration may differ among cell sources.

We recently identified a human primitive cell population consisting of cells we termed *monocyte-derived multipotential cells* (MOMCs), which show a fibroblast-like morphology in culture and have a unique molecular phenotype: they are positive for a monocytic marker, CD14; a hematopoietic marker, CD45; CD34 expressed

Contract grant sponsor: Japanese Ministry of Education, Science, Sports and Culture (to M.K.); Contract grant sponsor: Japanese Ministry of Health, Labor and Welfare (to M.K.); Contract grant sponsor: New Energy and Industrial Technology Development Organization of Japan (to M.K.).

*Correspondence to: Masataka Kuwana, Division of Rheumatology, Department of Internal Medicine, Keio University School of Medicine, 35 Shinanomachi, Shinjuku-ku, Tokyo 160-8582, Japan.
E-mail: kuwanam@z5.keio.jp

Received 25 January 2011; Revised 30 May 2011; Accepted 30 June 2011

Published online 4 November 2011 in Wiley Online Library (wileyonlinelibrary.com). DOI: 10.1002/jnr.22755

by endothelial cells and hematopoietic progenitors; and type I collagen (Kuwana et al., 2003). This cell type is generated by culturing peripheral blood MNCs on fibronectin in the presence of fetal bovine serum as the only source of exogenous growth factors. MOMCs are derived from circulating $CD14^+$ monocytes but can differentiate into several distinct mesenchymal cell types, including bone, cartilage, fat, and skeletal and cardiac muscle, similarly to mesenchymal stem cells (Kuwana et al., 2003; Kodama et al., 2005). In addition, human MOMCs can differentiate into the endothelial and neuronal lineages under the appropriate lineage-specific culture conditions (Kuwana et al., 2006; Kodama et al., 2006). Finally, MOMCs secrete a variety of cytokines and growth factors that are involved in tissue repair processes (Seta and Kuwana, 2010). This series of studies suggested that MOMCs are a potential transplantable cell source for use in tissue repair and regeneration.

In this study, we evaluated the beneficial effects of the intracranial transplantation of MOMCs in a rat model of ischemic stroke. We also examined the mechanisms underlying the potential benefits of MOMC delivery to ischemic lesions in the brain.

MATERIALS AND METHODS

Preparation of Rat MOMCs

Rat MOMCs were prepared as described for human MOMCs (Kuwana et al., 2003), with some modifications. Briefly, peripheral blood was obtained from the portal vein of male Sprague-Dawley (SD) rats (CLEA Japan, Tokyo, Japan) and subjected to Lymphoprep (Nycomed Pharma AS, Oslo, Norway) density gradient centrifugation. The MNCs were isolated and resuspended in low-glucose Dulbecco's modified Eagle's medium (DMEM) supplemented with 10% fetal bovine serum (JRH Bioscience, Lenexa, KS), 2 mM L-glutamine, 50 U/ml penicillin, and 50 μg/ml streptomycin. The cells were then spread at a density of 2×10^6/ml on fibronectin-coated plastic plates and cultured without any additional growth factors at 37°C. After 7 days of culture, adherent cells were collected as MOMCs and used for transplantation. In some experiments, circulating MNCs were cultured on uncoated plastic plates for 1 hr, and adherent and nonadherent cells were recovered separately for mRNA expression analysis. Macrophages were prepared by culturing adherent splenocytes on plastic plates in Medium 199 supplemented with 20% fetal bovine serum and 4 ng/ml macrophage colony-stimulating factor (R&D Systems, Minneapolis, MN) for 7 days. In some instances, MOMCs and macrophages were also prepared from transgenic male SD rats with an "enhanced" green fluorescent protein (GFP) cDNA, under the control of a chicken β-actin promoter and cytomegalovirus enhancer (Japan SLC, Hamamatsu, Japan; Ikawa et al., 1999). The phenotypic characteristics of rat MOMCs were evaluated by the following procedures (Kuwana et al., 2003).

Flow cytometric analysis. The cells were stained with fluorescein isothiocyanate-conjugated mouse anti-rat CD11b/Mac-1α monoclonal antibody (mAb; clone OX-42; Beckman Coulter, Fullerton, CA) or mouse anti-rat CD34 mAb (clone ICO115; Santa Cruz Biotechnology, Santa Cruz, CA), in combination with biotin-conjugated goat polyclonal antibodies to mouse IgG and streptavidin-PC5 (Beckman Coulter). Negative controls were cells incubated with an isotype-matched mouse mAb to an irrelevant antigen. The cells were analyzed on a FACSCalibur flow cytometer (BD Biosciences, San Diego, CA) using CellQuest software.

Uptake of acetylated low-density lipoprotein. The cells were labeled with 1,1′-dioctadecyl-3,3,3′,3′-tetramethylindocarbocyanine (Dil)-labeled acetylated low-density lipoprotein (acLDL; Molecular Probes, Eugene, OR) for 1 hr at 37°C and then analyzed by flow cytometry.

Immunocytochemistry. The cultured cells were fixed with formalin and incubated with the following primary antibodies: goat anti-rat CD45 polyclonal antibody (Santa Cruz Biotechnology), mouse anti-rat CD34 mAb, rabbit anti-rat collagen type I polyclonal antibody (Chemicon, Temecula, CA), and mouse anti-rat collagen type III mAb (clone FH-7A; Sigma, St. Louis, MO). Negative controls were cells incubated with normal goat IgG, normal rabbit IgG, or isotype-matched mouse mAb to an irrelevant antigen, instead of the primary antibody. Biotin-labeled anti-goat, -rabbit, or -mouse IgG antibodies combined with a streptavidin-horseradish peroxidase complex (Nichirei, Tokyo, Japan) were used for diaminobenzidine staining. Nuclei were counterstained with hematoxylin.

Analysis of mRNA expression. Total RNA was extracted from freshly prepared circulating MNCs, adherent MNCs, nonadherent MNCs, MOMCs, or bone marrow cells and subjected to cDNA synthesis using reverse transcriptase (Takara, Kyoto, Japan) with oligo-dT priming. The resulting cDNA (50 ng total RNA equivalent) was subjected to polymerase chain reaction (PCR) amplification using the following rat-specific primer pairs: CD14, 5′-GATCTGTCTGACAA CCCTGAGT-3′ (sense) and 5′-GTGCTCCTGCCCAGTG AAAGAT-3′ (antisense); collagen α1 type I, 5′-CTGGTGCT GCTGGTCGTGTT-3′ (sense) and 5′-TTGTTCGCCTGTC TCACCCT-3′ (antisense); and β-actin, 5′-AGGCATCCT GACCCTGAAGTAC-3′ (sense) and 5′-TCTTCATGAGG TAGTCTGTCAG-3′ (antisense). The primer sets for vascular endothelial growth factor (VEGF), angiopoetin-1 (Ang-1), placenta growth factor (PlGF), brain-derived neurotrophic factor (BDNF), and glial cell line-derived nerve growth factor (GDNF) were as described previously (Yamamoto et al., 2007; Torry et al., 2009; Zhao et al., 2011; Rodrigues et al., 2011). The PCR products were resolved by electrophoresis on 2% agarose gels and visualized by staining with ethidium bromide.

RAT MODEL FOR CEREBRAL ISCHEMIA

The model for cerebral ischemia was prepared by 1 hr of left middle cerebral artery occlusion (MCAO), followed by reperfusion, according to the method established by Belayev et al. (1996), with some modifications. Briefly, SD rats weighing 300–340 g were anesthetized with 2% isoflurane in a nitrous oxide/oxygen mixture (70%/30%) and maintained on this mixture during surgery. A midline surgical incision was made to expose the

left common, internal, and external carotid arteries. The distal portion of the external carotid artery was ligated, and the common and internal carotid arteries were temporarily blocked. A small incision was made in the proximal portion of the external carotid artery. A distal segment of a 4-0 nylon monofilament suture (Matsuda Ikakogyo, Tokyo, Japan) was coated with poly-L-lysine (Sigma) and Xantopren (Heraeus Kulzer, South Bend, IN) and inserted into the internal carotid artery to block the origin of the left middle cerebral artery. After 1 hr of MCAO, the intraluminal suture was carefully removed, and the neck incision was closed with silk thread. The rectal temperature was maintained between 36.5°C and 37.5°C using a thermostat-controlled heating pad during the surgical procedure. The animals were allowed to recover, with free access to food and water. This protocol was approved by the institutional Laboratory Animals Care and Use Committee, and all animal experiments were performed in accordance with the guidelines for animal experiments of Keio University School of Medicine.

MOMC Transplantation

Three groups of rats were given intracranial transplantations. One group received syngeneic MOMCs (10^7 cells/3 μl RPMI1640), one received syngeneic macrophages (10^7 cells/3 μl RPMI1640), and the control (mock-treated) group received 3 μl of RPMI1640 medium alone. For intracranial delivery, rats were reanesthetized 7 days after the MCAO procedure and subjected to stereotaxic injection of the cells into the striatum, adjacent to the ischemic core, as described previously (Suzuki et al., 2005). Figure 1a shows the site of injection: 1.0 mm posterior to the bregma, 3.0 mm lateral to the midline, and 7.0 mm ventral to the skull bone (Paxinos and Watson, 1998). In some instances, MOMCs and macrophages prepared from transgenic GFP-expressing syngeneic rats were used for the transplantations.

Magnetic Resonance Imaging

Rats were anesthetized and placed in a horizontal 7-Tesla animal magnetic resonance imager (PharmaScan 70/16; Bruker BioSpin).

Behavioral Tests

Rats underwent behavioral tests 1 week after MCAO and immediately before cell transplantation. The behavioral tests were repeated at 1, 2, 3, and 4 weeks after the transplantation. All rats were trained with three consecutive trials to generate stable baseline values before the MCAO procedure. All behavioral testing was performed and scored by the same experienced investigator (H.H.), who was blinded to the identity of the experimental group. The behavioral tests are described below.

Modified neurological severity score (mNSS). The mNSS is a composite of motor, sensory, balance, and reflex tests (Chen et al., 2001a), and neurological function was graded on a scale of 0–18 (Table I). Percentage severity in mNSS was calculated as the ratio of the scores at 1, 2, 3, and 4 weeks after transplantation divided by the score before transplantation.

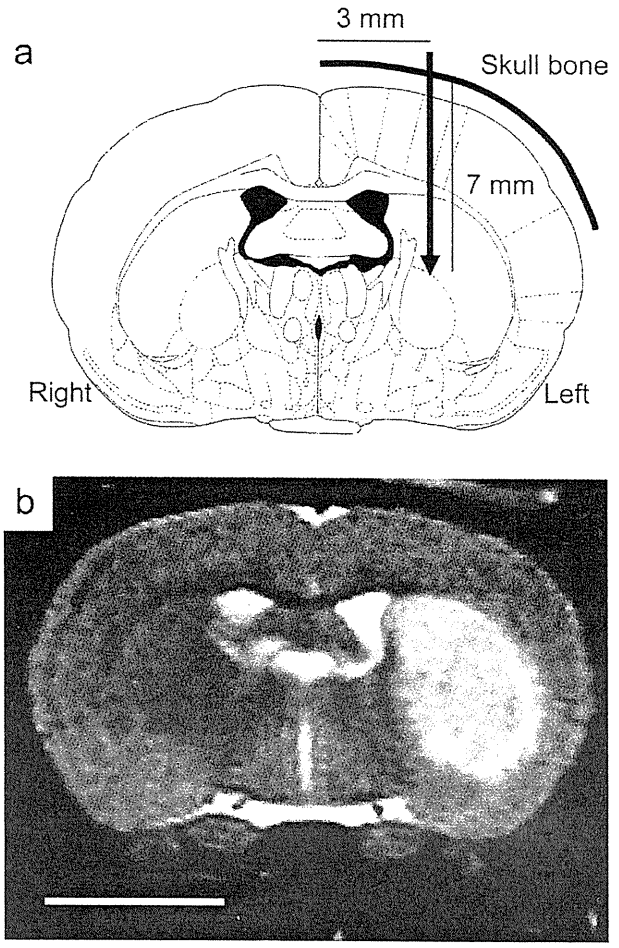

Fig. 1. Schematic diagram of the stereotaxic cell injection site and a magnetic resonance image taken 1 week after the MCAO procedure. **a:** Schematic diagram of a rat coronal brain section at the level of the striatum (1.0 mm posterior to the bregma). The vertical arrow indicates the needle track and the site of cell transplantation or medium injection. **b:** Coronal brain section generated by T2-weighted magnetic resonance imaging of a rat 1 week after MCAO. A representative image from one of five rats is shown. Scale bar = 5 mm.

Corner test. This procedure was performed as described previously (L. Zhang et al., 2002), with some modifications. The apparatus consists of two boards of 60 × 50 × 0.5 cm set at a 45° angle, so that the angle is perpendicular to the testing surface. A 1-cm opening is left between the boards to encourage the rat to enter the corner. A rat is placed between the two angled boards facing and halfway to the corner. When a rat attempts to enter the corner, the vibrissae on both sides of the head are stimulated simultaneously. The rat reacts

TABLE I. Modified Neurological Severity Score (mNSS)[a]

1. Motor tests (total 6)
Raising rat by tail (sum all items satisfied) subtotal 3
Flexion of forelimb 1
Flexion of hindlimb 1
Head moved >10° to vertical axis within 30 sec 1
Placing rat on floor (select one) subtotal 3
Normal walk 0
Inability to walk straight 1
Circling toward paretic side 2
Falls down to paretic side 3
2. Sensory tests (sum all items satisfied; total 2)
Visual and tactile test 1
Deep sensation (pushing paw against table edge to stimulate limb muscles) 1
3. Beam balance tests (select one; total 6)
Balances with steady posture 0
Grasps side of beam 1
Hugs beam and 1 limb falls down from beam 2
Hugs beam and 2 limbs fall down from beam, or spins on beam (>60 sec) 3
Attempts to balance on beam out but falls off (>40 sec) 4
Attempts to balance on beam out but falls off (>20 sec) 5
Falls off: no attempt to balance or hang on to beam (<20 sec) 6
4. Relax absence and abnormal movements (sum all items satisfied; total 4)
Pinna reflex (head shake when auditory meatus is touched) 1
Corneal reflex (eye blink when cornea is lightly touched with cotton) 1
Startle reflex (motor response to a brief noise from snapping) 1
Seizures, myoclonus, myodystony 1
Maximum points = 18

[a]13–18, severe injury; 7–12, moderate injury; 1–6, mild injury.

to the stimulation by rearing up (so that it can turn in the tight corner space) and turning, and it returns to all four paws facing the open end of the apparatus. Rats without ischemic injury turn either right or left with equal frequency, but rats that received the left MCAO procedure tended to turn toward the nonimpaired (left) side. Only turns involving full rearing along either board were recorded. Ten trials were performed for each rat, and the percentage of left turns was recorded as a measure of the severity of neurological damage.

Histological Assessments of the Brain

Sections of brain from the ischemic and contralateral sides were obtained at 1, 2, 3, and 4 weeks after transplantation. For sacrifice, the rats were transcardially perfused with ice-cold 0.9% saline solution and then with 4% paraformaldehyde/0.1 M phosphate-buffered saline. Frozen sections (20 μm) were prepared and stored at −80°C until use. Some sections were used for hematoxylin and eosin staining to assess tissue damage. A whole coronal brain section at the level of the striatum was recorded as an image under a digital microscope (VCR FRM20LZ; Omron, Kyoto, Japan), and infract sizes were evaluated in NIH Image. After endogenous peroxidases and nonspecific binding had been blocked with 1.5% skim milk, the sections were incubated overnight at 4°C with mouse anti-CD31 mAb (clone TLD-3AR; BD Biosciences). The slides were then reacted with an avidin-biotinylated enzyme complex system (DakoCytomation LSAB 2 system-HRP for use on rat specimens; Dako), and the immunoreactive signals were visualized with diaminobenzidine. To assess the specificity of the immunoreactivity, the primary antibody was omitted to provide a nonspecific control. The number of vessel-like structures or $CD31^+$ cells in a 0.25-mm^2 area was counted in 12 sections from four rats and is shown as the mean ± SD.

For fluorescent immunohistochemistry, the sections were incubated with mouse anti-CD31, anti-RECA-1 (clone HIS52; Serotec, Düsseldorf, Germany) or anti-NeuN mAb (clone A60; Chemicon), followed by incubation with mouse-specific IgG conjugated to AlexaFluor 568 and anti-GFP antibody conjugated to AlexaFluor 488 (Molecular Probes). Nuclei were stained with TO-PRO-3 (Molecular Probes), and the sections were examined with a confocal laser fluorescence microscope (Fluoview FV1000; Olympus, Tokyo, Japan).

Statistical Analysis

All variables are shown as the mean ± SD, and differences between two groups were examined by paired *t*-test. Serial changes were analyzed by repeated-measures analysis of variance (ANOVA). When a result reached significance ($P < 0.05$), post hoc tests were then carried out using Fisher's PLSD method. All statistical analyses were performed in Statview (version 5.0 for Windows; SAS Institute).

RESULTS

Establishment of Rat MOMCs

When the method for generating human MOMCs was applied to circulating MNCs from rats, the majority of adherent cells were spindle shaped (Fig. 2a). The majority of these cells were positive for a monocytic marker, CD11b/Mac-1α, and CD34 and were able to take up acLDL (Fig. 2b). Immunocytochemical analysis showed that the adherent cells expressed CD45, CD34, and type I and III collagens (Fig. 2c). Cells derived from five different rats showed the same characteristics.

We also prepared freshly isolated circulating MNCs, adherent and nonadherent MNCs (the adherent cells were obtained by the 7-day MOMC induction culture), and freshly isolated bone marrow cells from rats and subjected them to reverse transcription followed by PCR, to evaluate the expression of CD14 and type I collagen (Fig. 2d). We found that CD14 was markedly downregulated and that type I collagen was upregulated in the adherent cells obtained by the MOMC induction culture. Concordant findings were obtained in five independent experiments. These morphologic and phenotypic profiles of rat circulating MNC-derived adherent cells were unique and compatible with those of human MOMCs (Kuwana et al., 2003).

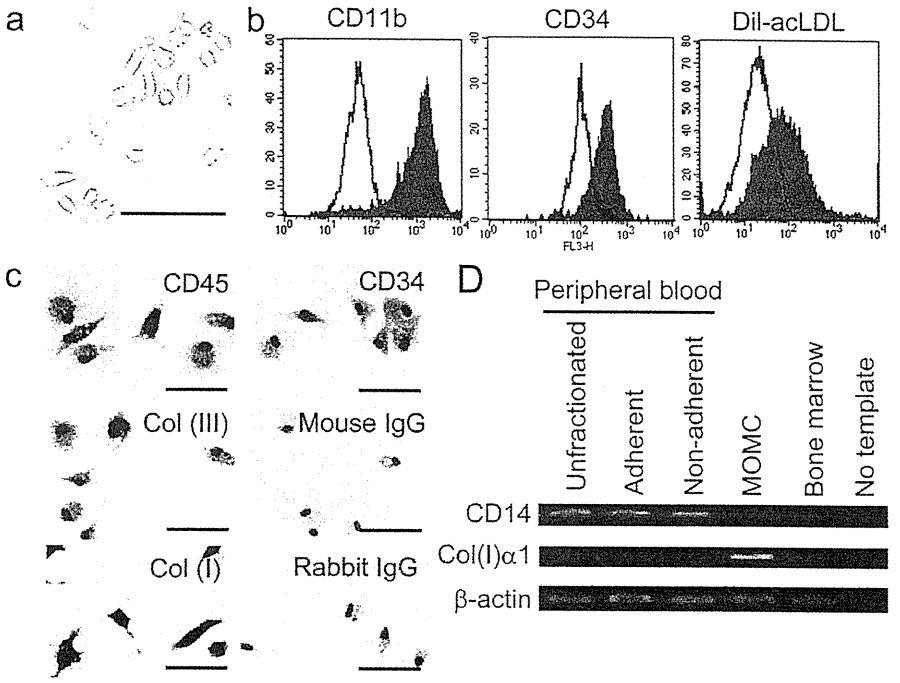

Fig. 2. Characterization of rat MOMCs. **a:** Phase-contrast images of cultured MOMCs. **b:** Flow cytometric analysis of MOMCs. Cells were stained with anti-CD11b or anti-CD34 mAbs or were cultured with Dil-acLDL and analyzed by flow cytometry. Expression or uptake of the molecules of interest is shown as shaded histograms. Open histograms represent staining with control antibody or mock treatment. **c:** Immunohistochemical analysis of MOMCs. Cells were stained with antibodies to the indicated cell-surface markers. Controls were incubated with control antibodies. Nuclei were counterstained with hematoxylin. **d:** PCR analysis to evaluate mRNA expression of CD14, type I collagen (Col[I]α1), and β-actin in freshly prepared MNCs, adherent MNCs, nonadherent MNCs, MOMCs, and bone marrow cells. Results shown are representative of five independent experiments. Scale bars = 100 μm in a; 50 μm in c.

Functional Recovery After Intracranial Transplantation of MOMCs

Rats that underwent left MCAO consistently showed right hemibody neurological deficits. Coronal brain sections generated by T2-weighted magnetic resonance imaging in a representative rat showed a hyperintense lesion in the middle cerebral artery territory (Fig. 1b), indicating the successful induction of left middle cerebral artery infraction. Only rats with severe neurological deficits showing both an mNSS > 6 and consistent turning to the left in the corner test 1 week after MCAO were used for the transplantation procedure.

In total 72 rats were assigned to one of three groups: the MOMC-transplanted group (n = 24), the macrophage-transplanted group (n = 24), and the mock-treated group (n = 24). The medium with or without cells was transplanted into the center of the ischemic site. All the animals survived to the planned endpoint and underwent serial neurological testing throughout the study.

The serial mNSSs demonstrated minimal functional recovery in all three groups 1 week after the transplantation (Fig. 3a). In the MOMC-transplanted rats, the mNSS severity tended to improve gradually until the 4-week endpoint, but the difference among the three groups never reached significance. The behavioral evaluation by the corner test also showed a trend toward functional recovery in all three groups (Fig. 3b). However, the MOMC-transplanted rats showed clear improvement at 3 weeks after the transplantation, which was greater than in the other two groups ($P = 0.02$). The post hoc analysis revealed a statistically significant difference in the percentage severity at 4 weeks after the transplantation: 70% ± 15% in the MOMC-transplanted group vs. 85% ± 11% in the macrophage-transplanted group or 89% ± 13% in the mock-treated group ($P = 0.04$ for both comparisons).

MOMC Transplantation Promoted Neovascularization in Ischemic Brain

The hematoxylin-eosin staining of brain sections showed massive necrosis in the ischemic core, and there was no difference in the infarct size among the three groups (Fig. 4). In the infarcted area of the cerebral cortex, especially in the ischemic boundary area, microvessel-like structures had appeared by 3 weeks after the transplantation, and their number increased dramatically thereafter in the MOMC-transplanted group (Fig. 5a), but almost none of these structures was detected in the

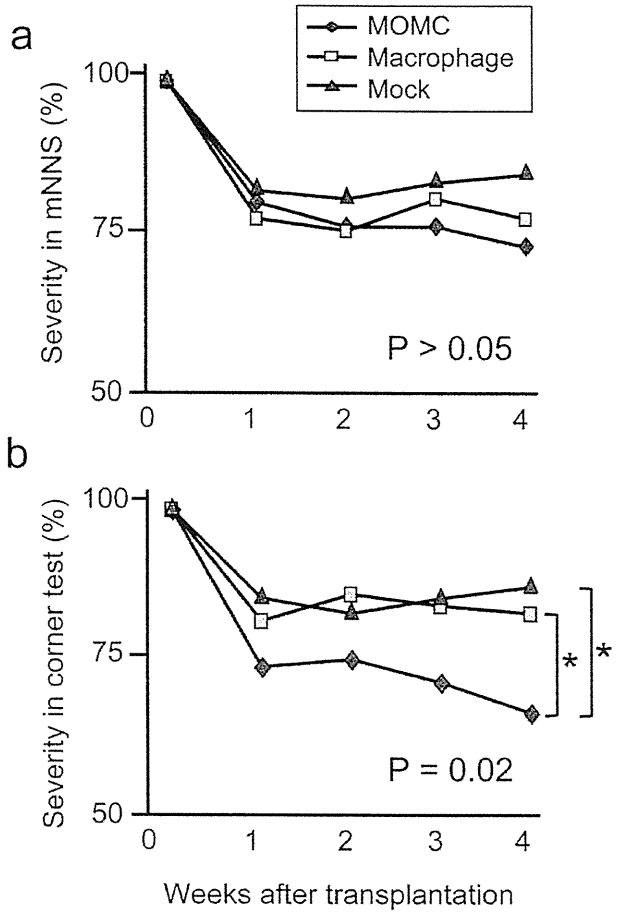

Fig. 3. Serial evaluations of rats after the MCAO procedure by mNSS (**a**) and the corner test (**b**) at 0 (pretransplantation), 1, 2, 3, and 4 weeks after cell transplantation. The mean value obtained from 24 rats in the MOMC-transplanted, macrophage-transplanted, and mock-treated groups is shown. The percentage severity in mNSS was calculated as the ratio of the scores at 1, 2, 3, and 4 weeks after transplantation divided by the score before transplantation. The percentage of left turns was recorded as the measure of severity in the corner test. An asterisk indicates a statistically significant difference by post hoc analysis.

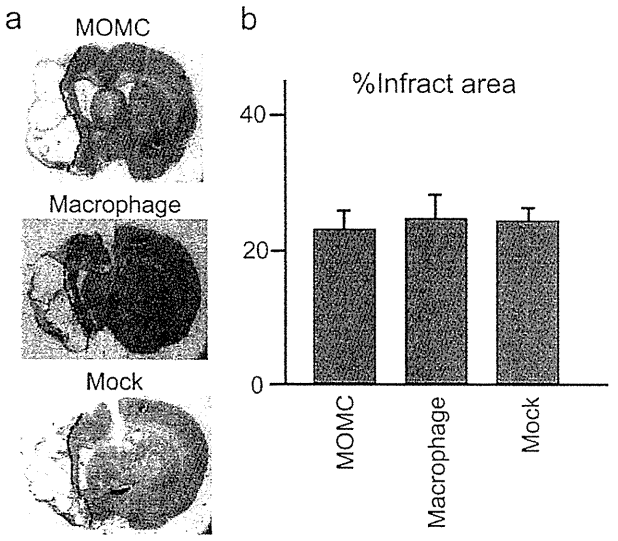

Fig. 4. Infarct sizes of whole coronal sections of MCAO rats after cell transplantation. **a:** Representative brain images of MOMC-transplanted, macrophage-transplanted and mock-treated rats at 4 weeks after transplantation. A dotted line denotes the ischemic boundary. **b:** Percentage infarct area in the whole-brain sections of MOMC-transplanted, macrophage-transplanted, and mock-treated rats at 4 weeks after transplantation. In total six sections were assessed for each group. The whole brain area and infract area were measured individually, and percentage infarct area was calculated based on a formula: infarct area divided by the whole brain area × 100. There was no statistical difference among three groups.

macrophage-transplanted or mock-treated group. At 4 weeks, the number of microvessel-like structures was significantly greater in the MOMC-transplanted group than in the macrophage-transplanted or mock-treated group (7.5 ± 1.6 vs. 3.1 ± 1.5 or 3.0 ± 1.3, $P < 0.01$ for both comparisons; Fig. 5b). When expression of CD31, also termed *platelet endothelial cell adhesion molecule-1*, was evaluated on the brain sections, large, round cells positive for CD31 were found in the ischemic boundary area of the MOMC-transplanted rats (Fig. 5c). These cells began to appear by 1 week after the transplantation; their numbers peaked at 2 weeks and decreased thereafter. Interestingly, these round $CD31^+$ cells were undetectable in the infarct lesions of mock-treated rats, but a small number was found at 2 and 3 weeks in the macrophage-transplanted rats. The number of round $CD31^+$ cells was significantly greater in the MOMC-transplanted group, compared with the macrophage-transplanted or mock-treated group, at 2 and 3 weeks after transplantation ($P < 0.01$ for all comparisons; Fig. 5d).

To evaluate further the fate of the transplanted cells in the ischemic brain, we used MOMCs and macrophages derived from syngeneic GFP-transgenic rats for cell transplantation (Fig. 6a). At 2 weeks after the transplantation, GFP-positive round cells were detected within the ischemic boundary of MOMC- and macrophage-transplanted rats, but their number was clearly greater in the MOMC-transplanted rats. The majority of GFP-positive cells were confirmed to express CD31, indicating that the round $CD31^+$ cells were derived from the transplanted MOMCs or macrophages. At 4 weeks posttransplantation, these GFP-positive transplanted cells had greatly decreased in number both in the MOMC-transplanted rats (Fig 6a, left), suggesting that the majority of these transplanted cells did not survive for 4 weeks. At high power, the cells surrounding the vascular structures clearly expressed both GFP and a mature endothelial marker, RECA-1 (Fig. 6a, right

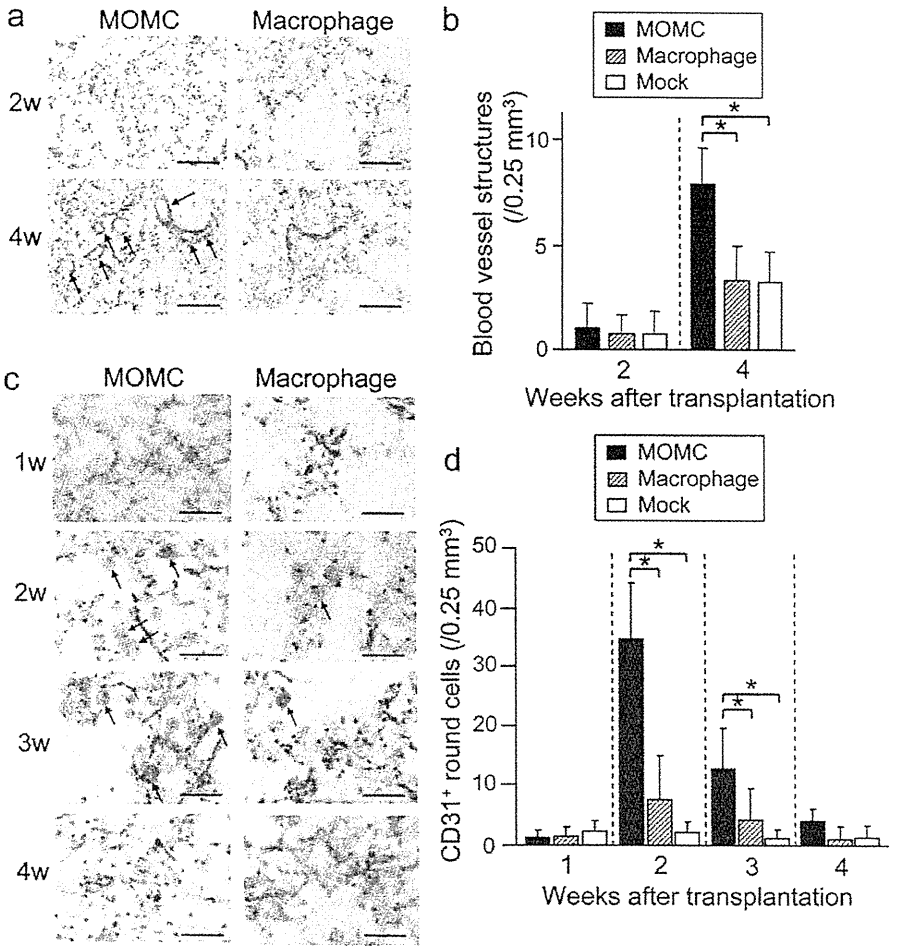

Fig. 5. Histological findings in brain sections of MCAO rats after cell transplantation. **a:** Representative hematoxylin-eosin-stained images in the infarcted cortex of MOMC- and macrophage-transplanted rats at 2 and 4 weeks after transplantation. Arrows indicate a blood vessel structure. **b:** The number of blood vessel structures in the infarcted cortex of MOMC-transplanted, macrophage-transplanted, and mock-treated rats at 2 and 4 weeks after transplantation. In total 12 sections from four rats were assessed for each group. $^*P < 0.01$. **c:** Representative images of CD31 immunostaining in the brain of MOMC- and macrophage-transplanted rats. Arrows indicate $CD31^+$ round cells. **d:** The number of $CD31^+$ round cells in the infarcted cortex of MOMC-transplanted, macrophage-transplanted, and mock-treated rats at 1, 2, 3, and 4 weeks after transplantation. In total 12 sections from four rats were assessed for each group. $^*P < 0.01$. Scale bars = 100 μm in a; 50 μm in c.

lower panel). Incorporation of GFP-positive cells into the endothelium was detected only in the MOMC-transplanted rats, suggesting that the transplanted MOMCs differentiated into mature endothelial cells. However, in sections derived from four MOMC-transplanted rats at 4 weeks, the proportion of endothelial cells expressing both GFP and RECA-1 in total GFP-positive cells was only 8%, and the majority of GFP-positive cells in the infarcted cortex remained the round $CD31^+$ cells. Moreover, only nine (18%) of 50 blood vessel-containing sections included GFP^+ endothelial cells, indicating that MOMC differentiation into endothelial cells was not a common event. Finally, none of the GFP-positive cells in the ischemic lesion of MOMC- or macrophage-transplanted rats expressed NeuN, a marker for mature neurons.

To examine further whether MOMCs were a source of angiogenic and neuroprotective factors, MOMCs, macrophages, and circulating MNCs were subjected to PCR to evaluate mRNA expression of selected factors associated with functional recovery in the brain (Johanson et al., 2011; Fig. 6b). MOMCs expressed a series of angiogenic factors, including VEGF, Ang-1, and PlGF. Especially strong expression of VEGF was relatively specific to MOMCs. On the other hand, expression of BDNF and GDNF was prominent in circulating MNCs, whereas expression of GDNF was also found in MOMCs but not in macrophages.

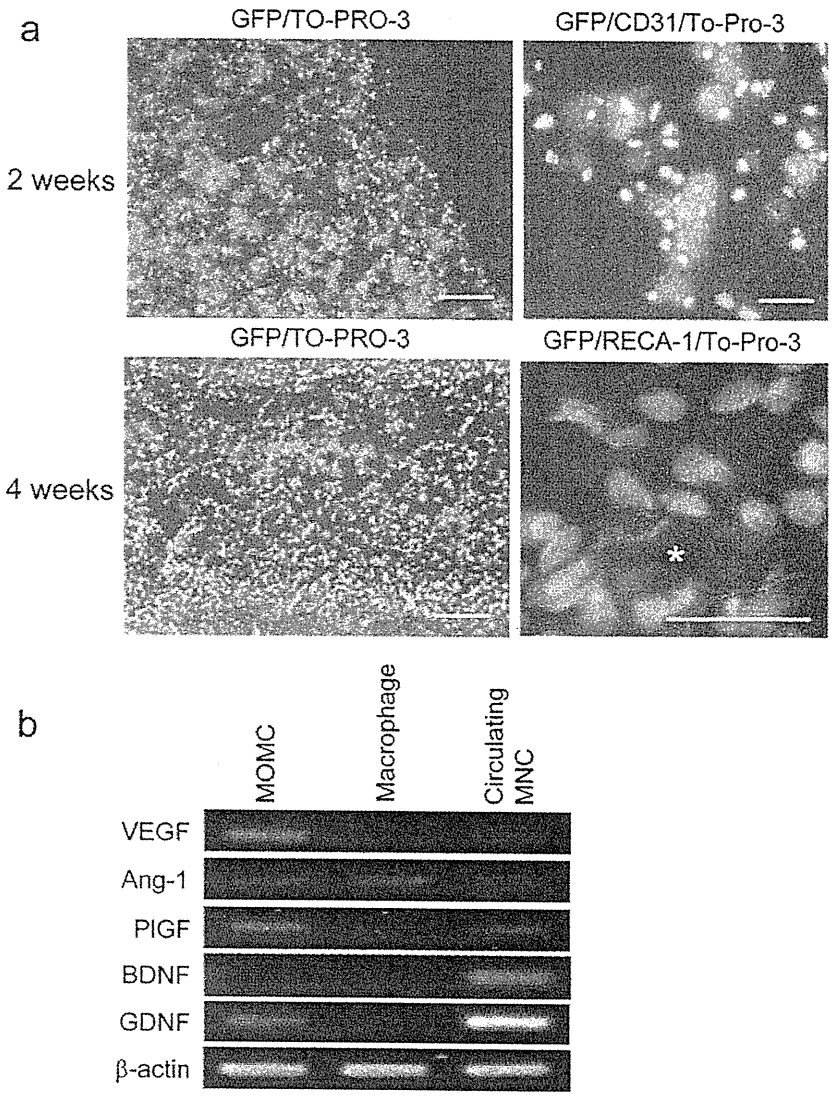

Fig. 6. Mechanisms of MOMC-mediated functional recovery in MCAO rats. **a:** Double immunostaining of brain sections of MCAO rats after the transplantation of GFP-transgenic rat-derived MOMCs. Representative immunofluorescent images in the ischemic boundary of MOMC-transplanted rats at 2 and 4 weeks after transplantation. Left panels are low-magnification images of immunostaining for GFP. Right panels show high-magnification images with double immunostaining for GFP and CD31 (top) or RECA-1 (bottom). Nuclei were counterstained with TO-PRO-3. An asterisk denotes a vascular lumen. **b:** PCR analysis to evaluate mRNA expression of VEGF, Ang-1, PlGF, BDNF, GDNF, and β-actin in MOMCs, macrophages, and circulating MNCs. Results shown are representative of five independent experiments. Scale bars = 25 μm in a, left; 100 μm in a, right.

DISCUSSION

In the present study, we successfully prepared a rat counterpart to human MOMCs. These cells showed a fibroblast-like morphology in culture and a unique molecular phenotype, positive for both hematologic and mesenchymal markers as well as CD34. In addition, intracranial transplantation of MOMCs 1 week after stroke reduced neurological deficits measured by the corner test in rats. The reduction in the functional impairment of the MOMC-transplanted rats could be explained by de novo vascularization in the infarct area, which was preceded by the appearance of MOMC-derived round $CD31^+$ cells. These findings provided evidence that MOMC-based cell therapy has potential efficacy for the treatment of ischemic stroke.

We detected the beneficial effect of MOMC transplantation on functional recovery by the corner test but not by the mNSS. This discrepancy may be attributable

to the different aspects of neurologic deficits evaluated by these behavioral tests. Specifically, the mNSS is composed of tests for a variety of neurological parameters, including alertness, motor functions, sensory functions, and reflexes (Chen et al., 2001a), and it is widely used for evaluating the most severe stroke conditions. In contrast, the corner test reflects sensory and motor asymmetries associated with cortical and striatal dysfunction and is often used to evaluate long-term functional deficits (L. Zhang et al., 2002). In fact, neurological recovery after bone marrow MNC transplantation was previously demonstrated in a rat model of cerebral ischemia by using the corner test (Brenneman et al., 2010).

In our protocol, MOMCs were transplanted 1 week after MCAO. This experimental protocol was designed to build in relevance to clinical application, because the preparation of MOMCs requires 1 week of culture. The administration of MOMCs immediately after cerebral ischemia may result in a more prominent reduction of ischemic brain injury, as reported in many rodent models for evaluating the effects of cell transplantation therapy (Chen et al., 2001a,b; Kamiya et al., 2008; Brenneman et al., 2010; Fan et al., 2010). However, other authors have reported that the therapeutic window for cell transplantation therapy is up to 1 month after stroke (Iihoshi et al., 2004; Shen et al., 2007b). Our study also differs from some others in that we chose an intracranial approach, to deliver cells directly into the ischemic lesion, because MOMCs administered via the circulation may not reach the lesion in sufficient numbers to repair massive injuries to the brain, owing to the damaged blood-supplying vessels. In addition, the intravenous delivery of bone marrow-derived cells was reported to result in loss of the cells from trapping by first-pass filters, such as the liver and lung (Chen et al., 2001a; Fischer et al., 2008). An intracarotid injection of MOMCs is another potential approach, but it was reported that the intraarterial delivery of bone marrow MNCs led to immediate deposition of the cells in the periinfarct area, but the majority of cells entered apoptosis immediately after migrating to the area of injury (Brenneman et al., 2010).

The mechanism underlying the MOMC-mediated functional recovery remains unclear. In this regard, MOMC transplantation did not decrease the infarct size, although this might have been due to the late timing of the transplantation. Moreover, we did not obtain any evidence that the transplanted MOMCs differentiated into neural cells, as described by Iihoshi et al. (2004) and Shyu et al. (2006). Instead, remarkable microvessel formation was observed in the ischemic boundary area at 4 weeks after the transplantation in the MOMC-transplanted rats; however, we did not confirm blood flow in these structures. Neovessel formation was preceded by an accumulation of MOMC-derived round $CD31^+$ cells in the infract area, which peaked 2 weeks after the transplantation, indicating that these MOMC-derived cells are likely to be involved in microvessel formation through at least two different processes. One possible mechanism is in vivo differentiation into mature endothelial cells and integration into the newly formed vasculature, because human MOMCs could differentiate into the endothelial cell lineage and contribute to vascular formation in vitro and in vivo (Kuwana et al., 2006). In this regard, vasculogenesis mediated by transplanted endothelial progenitor cells or neural stem cells was reported in several experimental ischemia models (Z.G. Zhang et al., 2002; Ii et al., 2009; Fan et al., 2010). However, our experiments using GFP-expressing MOMCs for transplantation revealed that the integration of MOMC-derived endothelial cells into the vascular wall was not a common event, suggesting that this mechanism does not solely play a role in the MOMC-mediated functional recovery.

On the other hand, human MOMCs produce a large variety of cytokines and growth factors that promote angiogenesis and tissue repair (Kuwana et al., 2006; Seta and Kuwana, 2010). In this study, we showed that rat MOMCs expressed a series of angiogenic factors, such as VEGF, Ang-1, and PlGF, which were shown to promote angiogenesis and functional recovery in an experimental stroke model (Liu et al., 2006; Onda et al., 2008 Hermann and Zechariah, 2009). Thus, transplanted MOMCs are likely to play a critical role in promoting the local angiogenesis governed by residential endothelial cells and progenitors through the secretion of a wide array of angiogenic factors. Especially the ability of MOMCs to express VEGF was greatly superior to macrophages, suggesting that this is partially responsible for the observed difference in functional recovery between rats receiving transplantation of MOMCs and rats receiving macrophages. Furthermore, GDNF produced by MOMCs may promote neuroregenerative and neuroprotective actions in the injured brain (Johanson et al., 2011). It is also possible that increased production of cytokines and growth factors in parallel to promotion of neovascularization can influence plasticity of stroke-damaged brain, insofar as GDNF has been shown to increase stroke-induced neurogenesis in an experimental stroke model (Kobayashi et al., 2006). Therefore, neovascularization through production of a large array of angiogenic factors in combination with in vivo differentiation into mature endothelial cells appears to be a primary mechanism for MOMC-mediated functional recovery in rat MCAO model.

In summary, our results with this clinically relevant rodent model indicate that MOMCs are a potentially effective candidate for use in cell transplantation therapy for cerebral ischemia. The ready collection of MOMCs from the peripheral blood makes them a safe and abundant source of autologous cells. Further studies are necessary to determine the optimal therapeutic timing and dose as well as method for delivery for MOMCs to be used clinically to treat ischemic stroke.

REFERENCES

Bang OY, Lee JS, Lee PH, Lee G. 2005. Autologous mesenchymal stem cell transplantation in stroke patients. Ann Neurol 57:874–882.

Belayev L, Alonso OF, Busto R, Zhao W, Ginsberg MD. 1996. Middle cerebral artery occlusion in the rat by intraluminal suture. Neurological and pathological evaluation of an improved model. Stroke 27:1616–1622.

Brenneman M, Sharma S, Harting M, Strong R, Cox CS Jr, Aronowski J, Grotta JC, Savitz SI. 2010. Autologous bone marrow mononuclear cells enhance recovery after acute ischemic stroke in young and middle-aged rats. J Cereb Blood Flow Metab 30:140–149.

Chen J, Li Y, Wang L, Zhang Z, Lu D, Lu M, Chopp M. 2001a. Therapeutic benefit of intravenous administration of bone marrow stromal cells after cerebral ischemia in rats. Stroke 32:1005–1011.

Chen J, Sanberg PR, Li Y, Wang L, Lu M, Willing AE, Sanchez-Ramos J, Chopp M. 2001b. Intravenous administration of human umbilical cord blood reduces behavioral deficits after stroke in rats. Stroke 32:2682–2688.

Fan Y, Shen F, Frenzel T, Zhu W, Ye J, Liu J, Chen Y, Su H, Young WL, Yang GY. 2010. Endothelial progenitor cell transplantation improves long-term stroke outcome in mice. Ann Neurol 67:488–497.

Fischer UM, Harting MT, Jimenez F, Monzon-Posadas WO, Xue H, Savitz SI, Laine GA, Cox CS. 2008. Pulmonary passage is a major obstacle for intravenous stem cell delivery: the pulmonary first pass effect. Stem Cells Dev 18:683–692.

Hermann DM, Zechariah A. 2009. Implications of vascular endothelial growth factor for postischemic neurovascular remodeling. J Cereb Blood Flow Metab 29:1620–1643.

Ii M, Nishimura H, Sekiguchi H, Kamei N, Yokoyama A, Horii M, Asahara T. 2009. Concurrent vasculogenesis and neurogenesis from adult neural stem cells. Circ Res 105:860–868.

Iihoshi S, Honmou O, Houkin K, Hashi K, Kocsis JD. 2004. A therapeutic window for intravenous administration of autologous bone marrow after cerebral ischemia in adult rats. Brain Res 1007:1–9.

Ikawa M, Yamada S, Nakanishi T, Okabe M. 1999. Green fluorescent protein (GFP) as a vital marker in mammals. Curr Top Dev Biol 44:1–20.

Johanson C, Stopa E, Baird A, Sharma H. 2011. Traumatic brain injury and recovery mechanisms: peptide modulation of periventricular neurogenic regions by the choroid plexus-CSF nexus. J Neural Transm 118:115–133.

Kamiya N, Ueda M, Igarashi H, Nishiyama Y, Suda S, Inaba T, Katayama Y. 2008. Intra-arterial transplantation of bone marrow mononuclear cells immediately after reperfusion decreases brain injury after focal ischemia in rats. Life Sci 83:433–437.

Kobayashi T, Ahlenius H, Thored P, Kobayashi R, Kokaia Z, Lindvall O. 2006. Intracerebral infusion of glial cell line-derived neurotrophic factor promotes striatal neurogenesis after stroke in adult rats. Stroke 37:2361–2367.

Kodama H, Inoue T, Watanabe R, Yasuoka H, Kawakami Y, Ogawa S, Ikeda Y, Mikoshiba K, Kuwana M. 2005. Cardiomyogenic potential of mesenchymal progenitors derived from human circulating $CD14^+$ monocytes. Stem Cells Dev 14:676–686.

Kodama H, Inoue T, Watanabe R, Yasutomi D, Kawakami Y, Ogawa S, Mikoshiba K, Ikeda Y, Kuwana M. 2006. Neurogenic potential of progenitors derived from human circulating $CD14^+$ monocytes. Immunol Cell Biol 84:209–217.

Kuwana M, Okazaki Y, Kodama H, Izumi K, Yasuoka H, Ogawa Y, Kawakami Y, Ikeda Y. 2003. Human circulating $CD14^+$ monocytes as a source of progenitors that exhibit mesenchymal cell differentiation. J Leukoc Biol 74:833–845.

Kuwana M, Okazaki Y, Kodama H, Satoh T, Kawakami Y, Ikeda Y. 2006. Endothelial differentiation potential of human monocyte-derived multipotential cells. Stem Cells 24:2733–2743.

Liu H, Honmou O, Harada K, Nakamura K, Houkin K, Hamada H, Kocsis JD. 2006. Neuroprotection by PlGF gene-modified human mesenchymal stem cells after cerebral ischaemia. Brain 129:2734–2745.

Onda T, Honmou O, Harada K, Houkin K, Hamada H, Kocsis JD. 2008. Therapeutic benefits by human mesenchymal stem cells (hMSCs) and Ang-1 gene-modified hMSCs after cerebral ischemia. J Cereb Blood Flow Metab 28:329–340.

Paxinos G, Watson C. 1998. The rat brain in stereotaxic coordinates,4th ed. New York: Academic Press.

Rodrigues DM, Li AY, Nair DG, Blennerhassett MG. 2011. Glial cell line-derived neurotrophic factor is a key neurotrophin in the postnatal enteric nervous system. Neurogastroenterol Motil 23:e44–e56.

Seta N, Kuwana M. 2010. Derivation of multipotent progenitors from human circulating $CD14^+$ monocytes. Exp Hematol 38:557–563.

Shen LH, Li Y, Chen J, Cui Y, Zhang C, Kapke A, Lu M, Savant-Bhonsale S, Chopp M. 2007a. One-year follow-up after bone marrow stromal cell treatment in middle-aged female rats with stroke. Stroke 38:2150–2156.

Shen LH, Li Y, Chen J, Zacharek A, Gao Q, Kapke A, Lu M, Raginski K, Vanguri P, Smith A, Chopp M. 2007b. Therapeutic benefit of bone marrow stromal cells administered 1 month after stroke. J Cereb Blood Flow Metab 27:6–13.

Shyu WC, Lin SZ, Chiang MF, Su CY, Li H. 2006. Intracerebral peripheral blood stem cell (CD34) implantation induces neuroplasticity by enhancing β1 integrin-mediated angiogenesis in chronic stroke rats. J Neurosci 26:3444–3453.

Suzuki S, Yamashita T, Tanaka K, Hattori H, Sawamoto K, Okano H, Suzuki N. 2005. Activation of cytokine signaling through leukemia inhibitory factor receptor (LIFR)/gp130 attenuates ischemic brain injury in rats. J Cereb Blood Flow Metab 25:685–693.

Torry RJ, Tomanek RJ, Zheng W, Miller SJ, Labarrere CA, Torry DS. 2009. Hypoxia increases placenta growth factor expression in human myocardium and cultured neonatal rat cardiomyocytes. J Heart Lung Transplant 2:183–190.

Yamamoto A, Takahashi H, Kojima Y, Tsuda Y, Morio Y, Muramatsu M, Fukuchi Y. 2007. Downregulation of angiopoietin-1 and Tie2 in chronic hypoxic pulmonary hypertension. Respiration 75:328–338.

Zhang L, Schallert T, Zhang ZG, Jiang Q, Arniego P, Li Q, Lu M, Chopp M. 2002. A test for detecting long-term sensorimotor dysfunction in the mouse after focal cerebral ischemia. J Neurosci Methods 117:207–214.

Zhang ZG, Zhang L, Jiang Q, Chopp M. 2002. Bone marrow-derived endothelial progenitor cells participate in cerebral neovascularization after focal cerebral ischemia in the adult mouse. Circ Res 90:284–288.

Zhao T, Li Y, Tang L, Li Y, Fan F, Jiang B. 2011. Protective effects of human umbilical cord blood stem cell intravitreal transplantation against optic nerve injury in rats. Graefes Arch Clin Exp Ophthalmol [E-pub ahead of print].

Int J Hematol (2011) 94:54–62
DOI 10.1007/s12185-011-0880-1

ORIGINAL ARTICLE

Mislocalization or low expression of mutated Shwachman–Bodian–Diamond syndrome protein

Masafumi Yamaguchi · Kingo Fujimura · Hirokazu Kanegane · Hanae Toga-Yamaguchi · Rajesh Chopra · Naoki Okamura

Received: 20 October 2010 / Revised: 17 May 2011 / Accepted: 19 May 2011 / Published online: 10 June 2011

Abstract Shwachman–Diamond syndrome (SDS) is an autosomal-recessive disorder characterized by exocrine pancreatic insufficiency and bone marrow failure. Mutations in the SBDS gene are identified in most patients with SDS. Recent studies have shown that SBDS is involved in ribosome biogenesis and is localized to the nucleolus. The significance of cellular localization in SBDS is unknown, particularly as SBDS does not exhibit canonical nuclear localization signals. In this study, we have constructed wild-type deletion mutants of the critical domains and disease-associated mutants of the SBDS gene. These constructs were expressed in HeLa cells to explore the subcellular distribution of normal and mutant proteins. Wild-type SBDS was detected in the nucleus. However, constructs lacking N-terminal Domain I and two disease-associated mutants (C31W and N34I) failed to localize SBDS to the nucleus. Moreover, the amount of mutated SBDS protein was decreased. When N-terminal Domain I was overexpressed in HeLa cells, the localization of endogenous SBDS protein was changed from nuclei to cytosolic fraction. These data indicate that the N-terminal Domain I is responsible for nuclear localization. Furthermore, low expression of SBDS, as exhibited in some of the disease-associated mutants, may be associated with the pathogenesis of SDS.

Keywords Bone marrow failure · Neutrophil · Neutropenia · Maturation · SBDS

Electronic supplementary material The online version of this article (doi:10.1007/s12185-011-0880-1) contains supplementary material, which is available to authorized users.

M. Yamaguchi (✉) · H. Toga-Yamaguchi · N. Okamura
Laboratory of Physiological Chemistry,
Hiroshima International University,
5-1-1 Hirokoshingai, Kure, Hiroshima 737-0112, Japan
e-mail: m-yamagu@ps.hirokoku-u.ac.jp

K. Fujimura
Laboratory of Clinicopathological Therapeutics,
Hiroshima International University, Kure, Japan

H. Kanegane
Department of Pediatrics, Graduate School of Medicine,
University of Toyama, Toyama, Japan

R. Chopra
Celgene Corporation, Summit, NJ, USA

1 Introduction

Shwachman–Diamond syndrome (SDS) is a rare autosomal-recessive disorder characterized by short stature, exocrine pancreatic insufficiency and bone marrow failure [1]. Neutropenia is the most common hematological manifestation in patients with SDS, although a subset of patients develops aplastic anemia and leukemia [2]. SDS is associated with mutations in the *SBDS* gene, which is a member of a highly conserved protein family in diverse species ranging from Archaea and yeast to vertebrate animals [3]. The *SBDS* gene is mapped to chromosome 7q11 and composed of five exons and encodes 250 amino acid residues [3]. The *SBDS* mRNA is widely expressed throughout in both human and murine tissue. In mice, SBDS protein has ubiquitous tissue expression [3, 4]. Taken together with multiorgan involvement in patients with SDS, the SBDS protein is likely to function in a variety of cellular processes. SBDS does not have any known sequence similarities, although orthologs are conserved across a number of species [3]. The structure of the *Archaeoglobus fulgidus* SBDS ortholog was solved,